Assessment of varying coupling levels between electric and thermal networks at district level using Co-simulation and model-predictive Control

Luca Rava, Audrey Wantier, Mathieu Vallee, Alain Ruby, Nicolas Lamaison

PROCEEDINGS OF ECOS 2022 - THE 35TH INTERNATIONAL CONFERENCE ON
EFFICIENCY, **C**OST, **O**PTIMIZATION, **S**IMULATION AND ENVIRONMENTAL IMPACT OF ENERGY SYSTEMS
3-7 JULY, 2022, COPENHAGEN, DENMARK

Assessment of Varying Coupling Levels between Electric & Thermal networks at District Level using Co-Simulation and Model-predictive Control

Luca Rava[a], Audrey Wantier[a], Mathieu Vallée[b], Alain Ruby[b] and Nicolas Lamaison[b]

[a] Université Grenoble Alpes, CEA, Liten, INES, *DTS*, 73375 Le Bourget du Lac, France, *firstname.lastname@cea.fr*

[b] Université Grenoble Alpes, CEA, Liten, INES, *DTCH*, 73375 Le Bourget du Lac, France, *firstname.lastname@cea.fr*

Abstract:

This study focuses on the co-simulation of the heating and electrical systems of a district. A heat pump, a gas boiler, a biomass cogeneration, a photovoltaic plant and the national electric grid provide electricity and heat consumed by thirteen residential buildings. Two storage units are present: a heat storage (hot water tank) and an electric storage (chemical battery). Architecture design and pre-sizing of components have previously been computed by MILP optimizations.

As part of the Trilogy platform, a co-simulation platform Pegase runs the grid control and the detailed physical models developed using Modelica (heat system) and Simulink (electric system). A model predictive control (MPC) based on sliding time window MILP optimisations manages the flexibility of the multi energy system and insures the balance between production and consumption. The objective of the optimizations is to minimise CO2 equivalent emission costs and operational costs of each component, including the purchase of gas, biomass and electricity.

A parametric study on the coupling strength between the electric and the heat system is performed by modifying the price of the electricity purchased from the national grid. Multiple scenarios with different thermoelectric coupling strength are analysed to show the dependency of the energy mix on the coupling strength. With increasing coupling, photovoltaic self-consumption increases and heat generation gradually shifts from the heat pump to the biomass cogeneration and to the gas boiler. This study also demonstrates how the Trilogy platform tools enable easy implementation of optimal control on co-simulations of multi energy detailed physical models.

Keywords: FMI, co-simulation, Model Predictive Control, energy storage, thermoelectric coupling, flexibility, modeling, complex energy system, district heating

1. Introduction

1.1. Context

In France and other countries, a large share of energy consumption is devoted to providing residential areas with space heating and domestic hot water preparation. While this demand has long been covered with fossil-fuels, it has to be quickly reduced in order to face challenges related to climate change, as well as for energy independence. Massive electrification of the residential sector, i.e., substituting fossil fuels with power-to-heat technologies, is one possible option for performing this shift, especially when considering renewable energy sources [1].

This transition process must take into account three major constraints. First, increasing the overall residential electricity consumption is not desirable. Indeed, a prospective study in France [1] recommends a slight decrease by 2050. Second, the temporal mismatch between renewable electricity production and consumption for residential purpose (especially at yearly scale) must be accounted for [2]. Third, thermal renovation of the existing building stock will take time and may not be phased with electrification and an increase of renewable production capacity. As a consequence, more realistic scenarios require not only electrification but also increased sector coupling, in particular between the electric and thermal networks, which can provide flexibility at different time scales (from instant to year) [3].

1.2. State of the art

Many works study sector coupling and multi-energy systems in the recent years. A typical categorization distinguishes between simulation, optimization and equilibrium methods [4]–[6]. Mavromatidis et al. [5] highlight that optimization models, although they are more widely used, are also less validated than simulation models.

The importance of fine-grained simulation for validating higher-level solution has been pointed out by Lamaison et al. [7], i.e. approximate models used for optimization can lead to different results or even infeasible cases in simulation.

Fine grained simulation of multi-vector district energy system poses modeling and performance challenges. In particular, no simulation tool is able to simulate all the domains with optimal efficiency, and the co-simulation approach has been proposed to overcome this challenge. Co-simulation is particularly relevant in studying multi-energy networks [8]–[10].

The choice of control strategies is also very important. It is very difficult to define rule-based control strategies that are capable to achieve the results obtained in optimization [10], [11], whereas Model-Predictive Control (MPC) control strategies for energy systems provide good results [9], [12], [13].

2. Case study: the Grenoble's "Cambridge" district

This paper considers a case study inspired on a real district in the city of Grenoble (France). This district, called the "Cambridge" district, has been studied in previous research work [14]–[16]. A complete description of the case can be found in the aforementioned papers: we briefly recall it here for the sake of completeness.

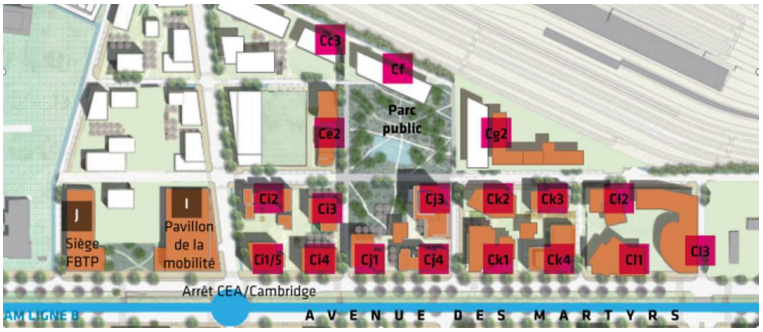

Fig. 1. Schematic representation of the "Cambridge" district (and its buildings) in the city of Grenoble, France. [16]

Fig. 1 [16] illustrates the layout of the "Cambridge" district. In this work, we consider 13 of its residential buildings, with approximately 500 dwellings.

2.1. Generation of electric and thermal load profiles

Based on the available data for these buildings (surface area, number of dwellings, monthly consumption), we used a combination of available load profile generation tools to produce synthetic load profiles at the hourly time step. More precisely, we combined:

- The CREST demand tool [17], [18], used for computing dynamic occupancy in each dwelling and for computing specific electricity demand profiles.
- A modified version of the DHW Calc tool [19] for computing Domestic Hot Water demand while taking into account occupancy profiles.
- A simplified dynamic thermal simulation model, defined in [20], for computing space heating profiles.

2.2. Hypotheses on energy and CO2 prices

The reference electricity price used in the simulations is based on the data available from the ENTSO-E Transparence platform [21]. This data has been adjusted with a constant bias in order to take into account transportation and distribution costs as well as the non-residential final consumer subscription. This constant bias is calculated in function of the average 2013-2018 values for France, retrieved from the Eurostat database [22]. The simulation's electricity price's yearly average value is 0.0758 €/kWh.

The prices for gas, biomass (wood) and CO_2 taxes are constant throughout the whole simulated year, as indicated in Table 1. The gas price is the maximum value retrieved from the Eurostat database [22] between 2013 and 2018, for non-residential consumers. Wood biomass price is retrieved from the IRENA report on renewable energy in District Heating and Cooling [23]. A CO2 tax of 100 €/t_{CO2} is assumed, although it has marginal impact on the results (only very high CO2 taxes above 250 €/t_{CO2} would change the results, however this is considered as an unrealistic value in the near future)

Table 1: gas, wood and CO2 equivalent emissions costs.

	Gas	Wood	CO_2
Cost	0.55 €/kg	0.12 €/kg	0.10 €/kg

CO_2 equivalent emissions costs only apply to heat production with gas and electricity extraction from the grid. The CO_2 emissions of burnt wood is considered zero because the same amount of CO_2 is assumed to be absorbed by the growth of new trees.

Gas CO_2 emissions have been estimated to be 0.243 kg_{CO2}/kWh. The CO_2 content of the electricity extracted from the grid is calculated from data of ENTSO-E [24] by applying CO_2 content data of the IPCC [25] to instantaneous power production. The average value of the electricity CO_2 content timeseries used in the simulations is 0.062 kg_{CO2}/kWh.

2.3. Multi-Energy System architecture

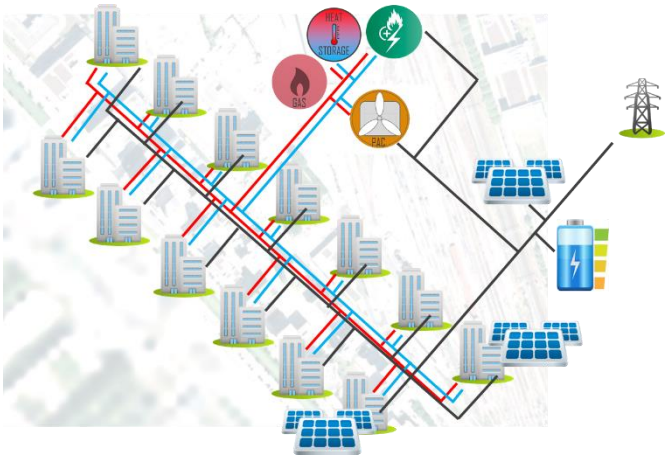

Fig. 2. Schematic representation of the multi-energy system architecture.

Fig. 2 gives a schematic representation of the multi-energy system architecture considered in this study. It features two energy distribution networks, the electricity distribution grid (in black) and the district heating network (in red and blue for supply and return lines). Note that the illustrated layout is not representative of the real district, and that the district heating network is not present in the actual district.

In this multi-energy system, various components can provide, convert or store energy either in electrical or thermal form. More specifically, we consider:

- Solar PV production and batteries at district level, as well as PV production at building level (rooftop)
- Heat pump, biomass cogeneration unit, backup gas boiler and heat storage at the district level

In particular, the heat pump and cogeneration units connected to the district heating network are two coupling points between the electric and thermal networks.

The photovoltaic production of the three plants included in the study is determined by data obtained from the PhotoVoltaic Geographical Information System (PVgis) online platform [27]. The panels' tilt was optimized by PVgis to the value of 36° in Grenoble's Cambridge neighbourhood. A perfect production forecast is used in the MPC control.

2.4. Sizing of production, conversion and storage components

The sizes of the production, conversion and storage components of the electrical and thermal parts of the district energy system were optimized from a techno-economic and environmental point of view using the PERSEE CEA software [11]. It provides a MILP library of models to write a classical unit commitment techno economical optimization problem, using a perfect one-year foresight assumption at hourly time-step.

The objective function is the Net Present Value of the system and accounts for Capex, Opex, purchase expenditures and carbon emission penalties for each component over 20 years of operation using a discount rate of 7%.

Besides technical and physical constraints, the installed power of the biomass cogeneration was limited at 360 kW to take into account the limited availability of wood and the regulations concerning the wood used for residential heating.

Another important constraint is the maximum limit of total yearly carbon emission mass, set at 20 t_{CO2}. This resulted in the absence of gas boiler, but a gas boiler was reintroduced for the simulations of this study because the detailed non linear thermal model requires it for its correct operation (the gas boiler represents the degree of freedom allowing to regulate flow and temperature of the heating fluid in the supply and return lines).

The decision variables to be optimized are:

- maximum production and storage capacities of the components
- hourly operating set points for each component

The table below shows the installed powers of each component.

Table 2. Sizing results.

	PV	Battery	Heat storage	Heat Pump	Cogeneration	Gas boiler
Sizing	7020 m^2	5600 kWh	11364 kWh	1268 kW	360 kW	1000 kW

The optimal values determined during this step depend on the one-year perfect foresight assumption: by over-estimating the capacity to anticipate future time evolution of boundary conditions, the optimization can underestimate the need for storage or production capacity. Hence, the final performance of a finer representation of the system could be worse than the one expected from the sizing step. Moreover, the present sizing based on the MILP formalism uses simplified linear description of the component behaviours, which is another possible important bias. It is also important to notice that during this sizing step only one optimization has been run on the whole horizon, while the moving shorter optimisation horizon used for the simulations ignores any event or data beyond its limited horizon.

3. Modelling

3.1. Methodological and Software frameworks

The TRILOGY platform is used to model the study case. It includes a simulation platform PEGASE that runs the different models: the electrical model developed with Simulink, the thermal model developed with Modelica and the control model called PERSEE. The electrical and thermal models are compiled as FMU models using the FMI-CS-2.0 standard [26].

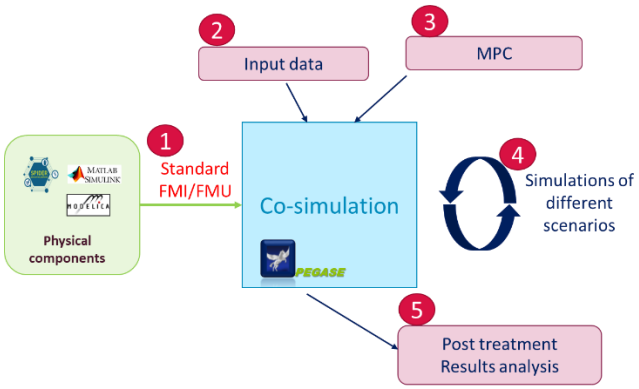

Fig. 3. General coupling scheme within PEGASE

The control of the energy system is performed by the PERSEE module of PEGASE, which implements the Model Predictive Control (MPC) of the system.

3.2. Electrical model

The electrical part of the physical model is controlled by power setpoints calculated in the optimization (battery) or calculated by the thermal model (heat pump and cogeneration). The former drives the physical model of the battery, the latter are taken into account in the energy balance calculation in order to know the electrical power supplied to or extracted from the grid. This model is developed with Simulink.

The electric consumption of the 13 buildings of the Cambridge neighbourhood is modelled with 13 simple load models. Among the 13 buildings, two have a PV installation on the roof. Another ground mounted PV power plant is included. These three PV power plants are modelled with a photovoltaic production model based on the conversion of solar irradiation into electrical power. An electrochemical battery and its inverter represent the electricity storage systems available in the microgrid. The electric grid is represented by the electrical power balance of all components of the study case. The heat pump power consumption and the biomass cogeneration electricity production are outputs of the thermal model and inputs of the electrical model. These setpoints are taken into account in the electrical power balance and produce the coupling of the thermal and electrical systems.

3.2.1. Buildings

The electrical load model makes use of a timeseries of consumed power and applies it to the building as its electrical consumption. These timeseries have been calculated based on statistical models of apartments' occupation and consumption of electrical devices, as specified in 2.1.

3.2.2. PV plants

The photovoltaic energy production model is driven by a solar irradiation timeseries perpendicular to the modules surface and a timeseries of air temperatures. The model calculates the AC electrical power produced by simulating the plant's inverter and the photovoltaic modules taking into account their working temperature.

3.2.3. Electrical storage

The electrical storage system is composed by two different models: the electrochemical battery and the inverter. The active power setpoint is an input of the inverter, which converts it into a current setpoint for the battery. The battery model uses an equivalent circuit model to calculate the real current flowing through its cells, the voltage and the electrical power. The current and the voltage are fed back as inputs to the inverter model to calculate the real power at the inverter's terminals.

Battery: it is a Li-Ion battery model with multiple parallel and series connected cells. It includes a BMS (Battery Management System) which saturates the battery setpoint according to the battery parameters. The cells physical model is based on an equivalent circuit model which simulates the electrical behaviour of the cells depending on the current setpoint and the working temperature.

Inverter: this model includes a control module which calculates the current setpoint for the battery and a physical module which calculates the AC power output of the inverter depending on the current and voltage information generated by the battery.

3.2.4. Electrical grid

The electrical grid is modelled with an electrical power balance of all the components included in the study case: this total is assumed to be balanced by the extraction or injection of power from or into the grid. Since the electrical losses of the grid and the time scale of its transients are negligible compared to the thermal system, this model is considered satisfactory for the study case of this paper.

3.3. Thermal model

The thermal model of the production plant is schematically illustrated in Fig. 4. The boundary conditions are the thermal output setpoints (Q) imposed to the generator by the controller (see Section 3.4) on one hand and the district heating network (DHN) setpoint departure temperature (Td_{DHN}), return temperature (Tr_{DHN}) and flow rate ($\dot{m}_{DHN}$) on the other hand. The latter boundary conditions account for DHW and space heating loads (see Section 2.1) and heat losses in the piping network (considered equal to 5%).

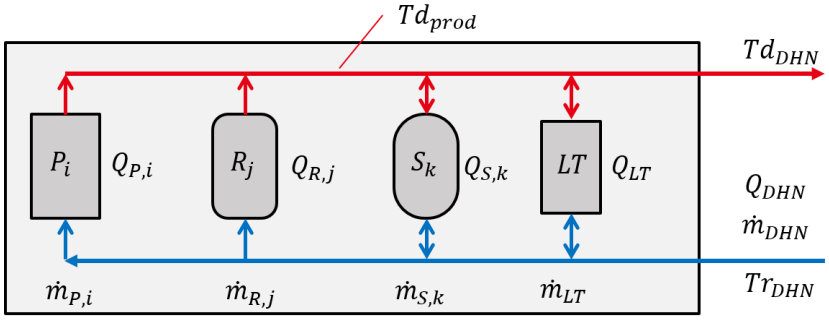

Fig. 4: Schematic representation of the model of the thermal network production plant

This generic model used for the present study is composed of 4 types of components, as highlighted in Fig. 4:

- Controllable generators (P_i) in which the output thermal power is controlled in order to satisfy the outlet setpoint temperature (T_{prod}), the mass flow rate is controlled in order to satisfy the external controller setpoint in terms of output thermal power. The operation is bounded by

maximum thermal output, flow rate and temperature. For the present study, the biomass cogeneration and the heat pump are operated in this way.

- Non-controllable generators (R_j) in which the thermal power is not-controlled and the flow rate is controlled in order to satisfy the outlet setpoint temperature. The operation is bounded by maximum flow rate and temperature. For the present study, there is no generator operated in this way but future studies may address a solar thermal field.
- Storages (S_k) in which the mass flow rate is controlled in order to satisfy the external controller setpoint in terms of thermal power. In case of charge, the flow rate is from top to bottom while in case of discharge, it is from bottom to top. The outlet temperature is floating and depending on the storage state. The operation is bounded by maximum flow rate. For the present study, the heat storage tank is operated in this way.
- The load-tracking generator (LT) in which the flow rate depends on the overall plant mass balance. When the resulting flow rate is from return to supply line, the generator thermal output power is controlled so that the outlet temperature of the plant is equal to the desired DHN departure temperature (Td_{DHN}). The operation is bounded by maximum thermal output, flow rate and temperature. For the present study, the gas boiler is operated in this way.

The physical models for all the components are based on static mass and momentum balances and dynamic energy balance. For the latter, input/output terms represent the convective transport, sources terms are heat loss and heat inputs, and accumulation terms represent the thermal inertia associated to fluid content and generator body. All the components are modelled without spatial discretization (0D modelling) except for storages in which 1D discretization along the fluid flow accounts for imperfect thermal stratification.

3.4. Control

The PEGASE tool allows to set up a Model-Predictive Control (MPC) managing the thermoelectric coupled energy system. The optimization problem is defined using a 24 hours horizon with perfect forecasts. Optimisations are performed with a timestep of 1 hour and are based on the same MILP models used during the sizing step (2.4). The differences between the optimization run during the sizing step and the moving horizon MPC optimizations included in the simulations of this study are:

- The optimisations are run at midnight every day with a horizon of 24 hours.
- The objective function is a pure operating cost function accounting for purchase expenditures (gas, wood, electricity) and carbon emission penalties.
- The decision variables are the hourly operating set points for each component: sizing variables are set to the optimal values determined in 2.4.

4. Simulations

In order to study the thermoelectric coupling effect on the energetic system, several simulations have been run on a horizon of one year with different grid electricity prices.

These prices can be indicators of the coupling strength between the electrical and thermal systems. Usually, in the case of a pure thermal simulation, the electricity needs are fulfilled through an electric grid without energy limits. This electricity extraction from the grid is considered as an operational cost of the thermal system analysed.

Instead, in the case of a thermoelectric co-simulation, the impact of the grid electricity supply on the system operation can be managed through an intelligent control of electrical and thermal components and measured with the use of detailed physical models. The electricity needs can be modulated or moved back or forward in time taking into account the controllable loads, the availability of the intermittent renewable energy and the storage capacity of the system. Because of the thermoelectric coupling, the system control can chose innovative ways to manage energy resources. The optimizer leans towards these types of energy management rather than the ones that are more dependent on an always available electricity source proportionally to the electricity price. In fact, when the electricity price of the grid is zero, there is no interest in storing energy, neither there is in favouring the self-consumption over the extraction of electricity from the grid: the electricity is simply extracted from the grid when the need arises. But when the electricity price is non-zero, the optimizer gradually favours other solutions over a limitless grid extraction and adopts different strategies depending on the electricity price.

This price timeseries has been modulated with a coefficient in order to run several simulations with different price magnitudes. Twelve simulations were run with twelve different price coefficients.

Table 3: List of simulations with the respective electricity price coefficient.

sim #:	1	2	3	4	5	6	7	8	9	10	11	12
coeff:	0	0.5	0.75	1	1.5	2	2.5	3	3.5	4	4.5	5

It is important to notice that the electricity price used in the simulations is only a purchase price, while the sale price is set to zero in order to favour self consumption.

The same timeseries of solar irradiation and temperature are used for all the simulations. This data has been retrieved from the PVgis online platform [27].

5. Results

The simulation results analysed are timeseries of electrical and thermal power actually produced or consumed by each detailed physical model of the study case. An example of operation is shown in Fig. 5.

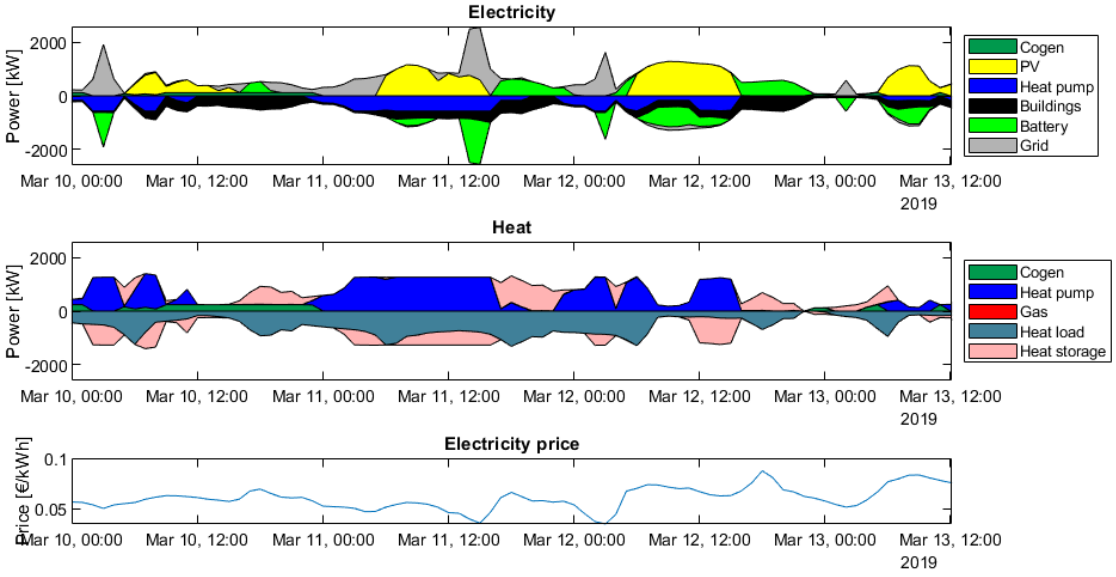

Fig. 5: Three days of operation of the electrical and thermal network of the Cambridge neighbourhood for an electricity price coefficient of 1 (original prices). Positive values are productions, negatives values are consumptions. "Heat Load" represents all thermal loads including losses.

Fig. 5 shows that the battery is often charged at night extracting energy from the electricity grid when the electricity price is lower, and discharged during the evenings, when the electricity price is higher. The battery is also recharged in case of abundance of photovoltaic production.

During the morning of second day of Fig. 5 (11th March) the photovoltaic production is enough to cover all electrical loads and is therefore stored into the battery. In the afternoon, the heat pump does not only satisfy the heat load, but recharges the heat storage too. This energy is then used during the evening, when both electrical and thermal loads are satisfied using stored energy.

It is worth noticing that the biomass cogeneration is only used during the day with low photovoltaic production (the first one of Fig. 5, 10th March). Wood is in fact used as the alternative renewable energy compensating the weak solar irradiation.

The simulation results have been analysed by calculating the yearly energy balance of each component and plotting it against the electricity price coefficient (Fig. 6).

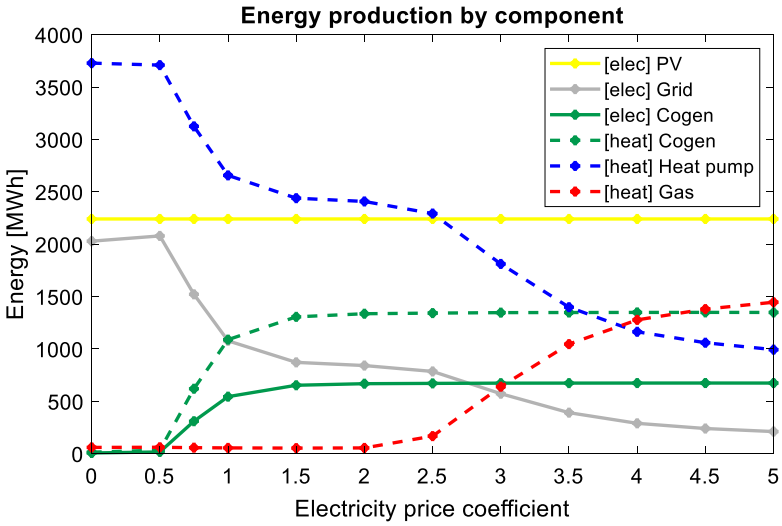

Fig. 6: Plot of yearly energy production of each component against the electricity price coefficient.

An electricity price of zero generates important electricity extraction from the grid. The photovoltaic power is self consumed thanks to the penalisation of the CO_2 emissions of the electricity extracted from the grid. It is only injected into the grid when all electrical and thermal charges are satisfied and when the storages are already charged. In all the cases where the photovoltaic power is not enough to supply the neighbourhood, remaining thermal and electrical needs are completely satisfied with electricity extraction from the grid. This electricity is either directly consumed, or stored in the battery or converted into heat with the heat pump. The generated heat is also either directly consumed either stored for later use. The flexibility provided by the electrical and thermal storages is used, in this case, to redistribute the photovoltaic production over the whole day and to buy the electricity when its CO_2 content is low. The biomass cogeneration and the gas boiler are never used.

At a normal electricity price (electricity price coefficient = 1) the biomass cogeneration allows to decrease the use of the heat pump and further decrease grid electricity extraction by providing both heat and electricity to the system. The cogeneration is often used during the winter, when the energy demand is higher, and only sometimes used in the summer, especially during the days when the photovoltaic production is low. Its installed power rarely covers all the energy demand, but it provides an often constant power output that helps reducing the electricity grid extraction through the use of storage systems and that allows the remaining electricity extractions to be limited to specific times when the electricity price is at a minimum.

At higher values of electricity prices a similar behaviour is observed, up to an electricity price coefficient of about 2.5. Another control strategy transition is observed between the electricity price coefficients 2.5 and 4. At these increasing values of the electricity price, heat production from gas becomes more and more viable. The heat pump production decreases according to the increase of heat produced by the gas boiler. At high electricity prices the heat pump is used most of the times with photovoltaic power. The flexibility provided by the electricity and heat storages is used to maximize self consumption and reduce electricity extraction from the grid. At even higher electricity prices (coefficient = 10) no significant deviation from the trend showed in Fig. 6 is observed: the energy mix tends to consolidate at constant values.

The electricity extracted from the grid between the two simulations with electricity price coefficients 0 and 0.5 seems to increase. This is the opposite phenomenon observed for higher electricity price coefficients and was not expected. However, an explanation can be found by looking at the total yearly battery losses of the two simulations in question. When the price coefficient is zero, extraction from the grid can happen at any time (except for the variable costs generated by the CO2 emission cost, which are on average small compared to half the electricity price: 0.0062 €/kWh versus 0.0379 €/kWh). Therefore, electrical loads can be satisfied with direct grid extraction most of the times and the use of the battery is very limited compared to all the other simulations. Instead, when all the variations of the electricity price create significant economic advantages to recharge the battery at very specific times,

the battery is used more often and, more importantly, with a higher charging power. Since electrical losses of the battery depend on the charging speed, this generates more electrical losses that cause the increase of grid electricity extraction observed between the first two simulations of Fig. 6 (coefficients 0 and 0.5). In order to analyse this phenomenon, the total yearly battery losses and the total yearly charged energy for each simulation have been plotted in Fig. 7. The losses have been normalized to the total yearly charged energy.

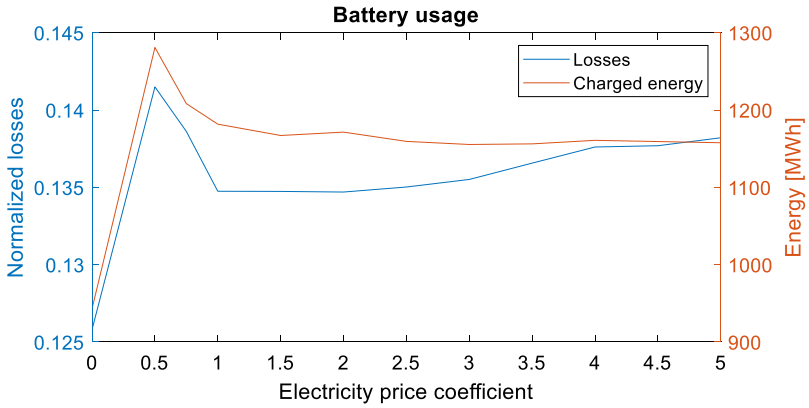

Fig. 7: Battery losses normalized to total charged energy and total charged energy against the electricity price coefficient.

As expected, normalized losses and use of the battery (total charged energy) increase from price coefficient 0 to price coefficient 0.5. Normalized losses then decrease again (though not as much) up to price coefficient 1. This can be explained with the introduction of the electrical production of the biomass cogeneration (Fig. 6). This generation reduces the overall need for electrical storage since it contributes to satisfy electrical demand during load peaks. The battery has to supply less energy during the peaks occurring at the same time as high electricity prices. It is therefore less charged when the electricity price is low and generates lower losses. For simulations with electricity price coefficient higher than 1, the electrical contribution of the biomass cogeneration to the system saturates and the use of the battery shows a slightly decreasing trend. The normalised battery losses increase again due to the exasperation of price differences: the charges are progressively more localized (therefore they are more often fast charges) at the times when the electricity price is low.

6. Conclusion and outlook

This study shows the ability of the TRILOGY platform to carry out co-simulations of electrical and thermal components controlled in the frame of the Model Predictive Control approach. It enables the full coupling of simplified linear electrical and thermal models to operate more detailed non-linear simulation models.

Sensitivity computations have been performed to assess the impact of the coupling strength between electrical and thermal models. Different control choices have been observed at different magnitudes of the electricity price, which suggest different behaviours of the electrical and thermal networks depending on their coupling strength. Specifically, the energy mix of the neighbourhood has been confirmed to be tightly related to the thermoelectric coupling strength.

This study highlights the importance of thermoelectric co-simulations in order to optimise energy use at a district level. The co-simulation platform developed for this study can be the basis of more advanced thermoelectric co-simulations of the same type. In particular, a comparison between simulations with and without detailed non linear models might generate important insights into their use in thermal-electric co-simulations. This is especially true when the forecasts used in the MPC control are not perfect and the optimised setpoints cannot be fully applied to the detailed physical models.

The analysis of the battery losses showed in Fig. 7 already generates an interesting insight into the way the battery is used even in the case of perfect forecasts. This analysis have been made possible by the use of a detailed non linear battery model that takes into account variable energy losses related to the speed of charge. This kind of insights rely on the use of detailed non linear models and can lead to the evaluation of innovative control rules and objectives and to better state of the art thermoelectric co-simulation expertise and results.

7. References

[1] RTE, 'Energy pathways 2050 - Key results'. Oct. 2021.

[2] A. Clerjon and F. Perdu, 'Matching intermittent electricity supply and demand with electricity storage - An optimization based on a time scale analysis', *Energy*, vol. 241, 2022, doi: 10.1016/j.energy.2021.122799.

[3] A. Vandermeulen, B. van der Heijde, and L. Helsen, 'Controlling district heating and cooling networks to unlock flexibility: A review', *Energy*, vol. 151, pp. 103–115, May 2018, doi: 10.1016/j.energy.2018.03.034.

[4] H.-K. Ringkjøb, P. M. Haugan, and I. M. Solbrekke, 'A review of modelling tools for energy and electricity systems with large shares of variable renewables', *Renewable and Sustainable Energy Reviews*, vol. 96, pp. 440–459, Nov. 2018, doi: 10.1016/j.rser.2018.08.002.

[5] G. Mavromatidis *et al.*, 'Ten questions concerning modeling of distributed multi-energy systems', *Building and Environment*, vol. 165, p. 106372, Nov. 2019, doi: 10.1016/j.buildenv.2019.106372.

[6] E. Cuisinier, C. Bourasseau, A. Ruby, P. Lemaire, and B. Penz, 'Techno-economic planning of local energy systems through optimization models: a survey of current methods', *International Journal of Energy Research*, vol. 45, no. 4, pp. 4888–4931, 2021, doi: https://doi.org/10.1002/er.6208.

[7] N. Lamaison, S. Collette, M. Vallée, and R. Bavière, 'Storage influence in a combined biomass and power-to-heat district heating production plant', *Energy*, vol. 186, p. 115714, Nov. 2019, doi: 10.1016/j.energy.2019.07.044.

[8] B. Leitner, E. Widl, W. Gawlik, and R. Hofmann, 'A method for technical assessment of power-to-heat use cases to couple local district heating and electrical distribution grids', *Energy*, vol. 182, pp. 729–738, Sep. 2019, doi: 10.1016/j.energy.2019.06.016.

[9] M. Vallée *et al.*, 'An efficient co-simulation and control approach to tackle complex multi-domain energetic systems: concepts and applications of the PEGASE platform', presented at the Proc. of the 32th Int. Conf. on Efficiency, Cost, Optimization, Simulation and Environmental Impact of Energy Systems (ECOS), Jun. 2019.

[10] M. Descamps, N. Lamaison, M. Vallée, and R. Bavière, 'Operational Control of a Multi-energy District Heating System: Comparison of Model-Predictive Control and Rule-Based Control', presented at the Proc. of the 32th Int. Conf. on Efficiency, Cost, Optimization, Simulation and Environmental Impact of Energy Systems (ECOS), Jun. 2019.

[11] É. Cuisinier, P. Lemaire, B. Penz, A. Ruby, and C. Bourasseau, 'New rolling horizon optimization approaches to balance short-term and long-term decisions: An application to energy planning', *Energy*, vol. 245, p. 122773, Apr. 2022, doi: 10.1016/j.energy.2021.122773.

[12] B. Leitner, E. Widl, W. Gawlik, and R. Hofmann, 'Control assessment in coupled local district heating and electrical distribution grids: Model predictive control of electric booster heaters', *Energy*, vol. 210, p. 118540, Nov. 2020, doi: 10.1016/j.energy.2020.118540.

[13] E. Saloux and J. A. Candanedo, 'Model-based predictive control to minimize primary energy use in a solar district heating system with seasonal thermal energy storage', *Applied Energy*, vol. 291, p. 116840, Jun. 2021, doi: 10.1016/j.apenergy.2021.116840.

[14] C. Pajot, N. Artiges, B. Delinchant, S. Rouchier, F. Wurtz, and Y. Maréchal, 'An Approach to Study District Thermal Flexibility Using Generative Modeling from Existing Data', *Energies*, vol. 12, no. 19, p. 3632, Jan. 2019, doi: 10.3390/en12193632.

[15] J. Fitó *et al.*, 'Energy- and exergy-based optimal designs of a low-temperature industrial waste heat recovery system in district heating', *Energy Conversion and Management*, vol. 211, p. 112753, May 2020, doi: 10.1016/j.enconman.2020.112753.

[16] J. Fitó, M. Vallée, A. Ruby, and E. Cuisinier, 'Robustness of District Heating versus Electricity-Driven Energy System at District Level: a Multi-Objective Optimization Study', *Smart Energy (submitted)*, 2022.

[17] I. Richardson, M. Thomson, and D. Infield, 'A high-resolution domestic building occupancy model for energy demand simulations', *Energy and Buildings*, vol. 40, no. 8, pp. 1560–1566, 2008, doi: 10.1016/j.enbuild.2008.02.006.

[18] I. Richardson, M. Thomson, D. Infield, and C. Clifford, 'Domestic electricity use: A high-resolution energy demand model', *Energy and Buildings*, vol. 42, no. 10, pp. 1878–1887, Oct. 2010, doi: 10.1016/j.enbuild.2010.05.023.

[19] U. Jordan and K. Vajen, 'DHWcalc: program to generate domestic hot water profiles with statistical means for user defined conditions', Orlando (US), Aug. 2005.

[20] N. Aoun, R. Bavière, M. Vallée, and G. Sandou, 'Development and assessment of a reduced-order building model designed for model predictive control of space-heating demand in district heating systems', Jun. 2019.

[21] ENTSOE Transparency platform, 'Day Ahead Prices (hourly data for 2018 on bidding zone FR)', 2018. https://transparency.entsoe.eu/transmission-domain/r2/dayAheadPrices/show (accessed Mar. 09, 2022).

[22] EUROSTAT, 'Electricity prices by type of user [TEN00117]'. https://ec.europa.eu/eurostat/databrowser/bookmark/a380caa8-545b-4665-a78e-86f63df6b3ed?lang=en

[23] IRENA, 'ANNEX 4: FUEL COSTS', in *Renewable Energy in District Heating and Cooling, A sector roadmap for REmap*, International Renewable Energy Agency, Abu Dhabi., IRENA, 2017, p. 85. [Online]. Available: https://www.irena.org/publications/2017/Mar/Renewable-energy-in-district-heating-and-cooling

[24] ENTSOE Transparency platform, 'Actual Generation per Production Type (hourly data for 2018 on bidding zone FR)', 2018. https://transparency.entsoe.eu/generation/r2/actualGenerationPerProductionType/show

[25] Intergovernmental Panel on Climate Change, 'Technology-specific Cost and Performance Parameters', in *Climate Change 2014: Mitigation of Climate Change: Working Group III Contribution to the IPCC Fifth Assessment Report*, Cambridge University Press, 2015, pp. 1329–1356. doi: 10.1017/CBO9781107415416.025.

[26] FMI development group, 'Functional Mock-up Interface 2.0.3 specifications', Nov. 2021. [Online]. Available: https://github.com/modelica/fmi-standard/releases/download/v2.0.3/FMI-Specification-2.0.3.pdf

[27] EU science hub, 'PhotoVoltaic Geographical Information System (PVgis), hourly data at the Cambridge's Grenoble neighbourhood, .', 2019. http://re.jrc.ec.europa.eu/pvg_tools/fr/tools.htm